

# Methods

Cite this: *Anal. Methods*, 2011, **3**, 849[www.rsc.org/methods](http://www.rsc.org/methods)

PAPER

## SERS labels for quantitative assays: application to the quantification of gold nanoparticles uptaken by macrophage cells

Vincenzo Amendola,<sup>\*a</sup> Moreno Meneghetti,<sup>a</sup> Stefania Fiameni,<sup>b</sup> Stefano Polizzi,<sup>c</sup> Giulio Fracasso,<sup>d</sup> Anita Boscaini<sup>d</sup> and Marco Colombatti<sup>d</sup>

Received 1st November 2010, Accepted 28th January 2011

DOI: 10.1039/c0ay00660b

Labels based on noble metal nanoparticles and surface enhanced Raman scattering (SERS) opened new opportunities for the ultrasensitive detection of analytes. To date, however, SERS labels were mostly used for qualitative analysis, while leaving largely unexploited their potential for ultrasensitive quantitative assays. Here we synthesized SERS labels based on gold nanoparticles (AuNPs) obtained by laser ablation synthesis in solution and we developed a general method for the correlation of the SERS label concentration with the intensity of the Raman signal. We successfully used this method for the quantification of the number of AuNPs uptaken by PMA differentiated U937 macrophage cells. Our work shows that quantitative ultrasensitive assays by SERS labels are possible and points out some issues that must be considered when performing this type of analysis.

### Introduction

The demand for ultrasensitive identification and quantification of analytes has greatly increased over the past few years.<sup>1–3</sup> For instance, the study and the diagnosis of complex diseases where many different biomarkers are present, like cancer, have a great need for analytical techniques with these characteristics.<sup>1,2,4</sup> Nanoscale engineered materials can provide new solutions to this problem. In particular, biolabelling based on surface enhanced Raman scattering (SERS) is one of the most promising techniques for ultrasensitive assays.<sup>5–10</sup> Usually, Raman scattering shows weak signals compared to Rayleigh scattering or fluorescence, but when molecules are adsorbed on the surface of metallic nanostructures with plasmonic properties, a huge enhancement of the differential Raman scattering cross-section, that can be of the order of  $10^{14}$  in best cases, is observed.<sup>5,11–15</sup> Such an enhancement derives in particular from the local electric field enhancement due to the surface plasmon resonance of the metal nanostructure (electromagnetic enhancement), and to the charge transfer processes involving electron transfer between the molecule and the metal substrate (chemical enhancement).<sup>12,13,16</sup> Most intense signals are obtained when also the molecule is in resonance with the laser excitation, namely in the

case of surface enhanced resonant Raman scattering (SERRS).<sup>13,16,17</sup> SERS labels can be a valid alternative to fluorescent tags based on organic fluorophores or semiconductor quantum dots because they show some important peculiarities. In particular the bandwidth of Raman peaks is on the order of few nm that is much narrower than fluorescence emission bands.<sup>4,6,18</sup> This property and the distinctive Raman fingerprint of different molecules allow the development of a wide series of SERS labels with a distinctive spectral signature.<sup>4,6</sup> Multiple labels can be excited at the same time with the same laser wavelength, giving to SERS labels a great potential for multiplexed analysis.<sup>4,6,19</sup> Moreover, SERS signals are suited for long time observation because they do not show photobleaching, while blinking cycles occur on a timescale of fractions of seconds and are important only in the case of single molecule analysis.<sup>5</sup> An important difference with fluorescence is that Raman is not sensitive to the background, contrary to what happens with fluorescent labels due to autofluorescence, and, especially in the near infrared spectral window, SERS labels can be also brighter than semiconductor quantum dots.<sup>5,11,18</sup> Therefore, higher sensitivity and lower detection limits than ordinary fluorescent tags are usually expected.<sup>4–6</sup> Several bright examples about the application of SERS labels in nanobiotechnology and nanomedicine have been reported in recent years and various SERS labels have been developed.<sup>18,20–38</sup> For instance, gold nanoparticles capped with thiol terminated oligonucleotides composed of a Raman active molecule on the inner end and a DNA capture sequence have been used for the multiplexed detection of femtomolar amounts of more than six different DNA sequences in the same microarray.<sup>20</sup> In an analogous microarray set up, gold nanoparticles (AuNPs) with a targeting

<sup>a</sup>Department of Chemical Sciences, University of Padova, via Marzolo 1, I-35131 Padova, Italy. E-mail: [vincenzo.amendola@unipd.it](mailto:vincenzo.amendola@unipd.it)

<sup>b</sup>CNR—IENI, Corso Stati Uniti 4, 35127 Padova, Italy

<sup>c</sup>Department of Molecular Sciences and Nanosystems, Università Ca' Foscari Venezia and INSTM UdR Venezia, via Torino 155/b, I-30172 Venezia-Mestre, Italy

<sup>d</sup>Department of Pathology and Diagnostic, Section of Immunology, University of Verona, P.le LA Scuro 10, I-37134 Verona, Italy

protein allowed the ultrasensible detection of proteins.<sup>21</sup> Silver nanoparticles coated with aptamers allowed the detection of thrombin and other target proteins with high selectivity and sensitivity in a microarray configuration.<sup>23</sup>

Although a variety of SERS labels were developed until now,<sup>18,20–38</sup> they have been used for qualitative analysis. Quantitative analysis based on SERS labels can be a new interesting analytical chemistry technique,<sup>1,2,6,26,39–41</sup> but requires the development of an effective methodology for the quantification of SERS labels by the intensity of their Raman signal.

Here we show that it is possible to correlate accurately the SERS signal with the concentration of SERS labels based on AuNP. Our method consists in the evaluation of the concentration of SERS labels by fitting their UV-visible absorption spectra with a Mie–Gans model, according to a well established procedure previously reported.<sup>42</sup> The results show that a linear correlation between the AuNP concentration and the SERS signals is found. The fitting program can be freely downloaded from the web. Therefore, our method requires an UV-visible spectrometer, a Raman spectrometer and a personal computer. We successfully applied our method to the determination of the number of AuNP uptaken by macrophage cells and we found a good correlation with the results of more demanding techniques like inductively coupled plasma-mass spectrometry (ICP-MS). We also found that the choice of an appropriate calibration curve is important for the accuracy of the assay.

## Experimental methods

### Preparation and characterization of SERS labels

AuNPs with average size of 19 nm were obtained by laser ablation synthesis in solution (LASiS), as previously reported.<sup>43–45</sup> Laser ablation uses Nd:YAG (Quantel YG981E) laser pulses at 1064 nm (9 ns) focused with a 10 cm focus lens on a 99.9% pure gold plate placed at the bottom of a cell containing a  $10^{-5}$  M NaCl solution in bidistilled water. Pulses of  $10 \text{ J cm}^{-2}$  at 10 Hz repetition rate for 90 min were employed. Freshly prepared Raman active dye solutions (1 mM in ethanol or in water) were added to a 2 nM AuNP solution at a 1 : 100 volume ratio. The following dyes were used: methylene blue (BM, trihydrate, Sigma-Aldrich); cresyl violet 670 (CV, Perchlorate, Exciton); hexacyanin 3 (HITC, Perchlorate, Exciton); malachite green (MG, oxalate salt, Sigma-Aldrich); malachite green isothiocyanate (MGITC, Invitrogen); Nile blue A (NB, sulfate, Sigma-Aldrich); oxazine 750 (OX, perchlorate, Exciton); and tetramethylrhodamine isothiocyanate (TRITC, mixed isomers, Sigma-Aldrich). After 30 minutes under mild stirring, a freshly prepared aqueous solution of thiolated polyethylene glycol (PEG,  $M_w$  5000, Lysan Bio) was added to AuNP with a ratio of 15 000 PEG molecules for each nanoparticle. The mixtures were maintained under mild stirring for 12–14 hours at room temperature. After incubation, the suspensions were washed several times by centrifugation at 5000 rpm for 10 minutes. At the end of the washing procedure, all solutions were filtered with hydrophilic  $0.45 \mu\text{m}$  cellulose filters. The presence of PEG on the surface of AuNP is evident because it provided excellent stability to AuNP in physiological medium, contrary to the fast particles aggregation and precipitation observed for uncoated AuNP.

Moreover, the red shift of the plasmon band (*ca.* 3 nm) was observed on AuNP coated with PEG with respect to pristine AuNP. All Raman labels were obtained with the same procedure described above.

AuNPs were characterized both by UV-visible spectroscopy using a Varian Cary 5 spectrometer in 2 mm optical path quartz cells, and by transmission electron microscopy (TEM) collecting images at 300 kV with a JEOL JEM 3010 microscope equipped with a Gatan Multiscan CCD Camera model 794. The samples for TEM analysis were prepared by evaporating AuNP suspension on a copper grid covered with an amorphous carbon holey film.

Z-Spectroscopy measurements were performed with a Spectra Physics Nicomp 380 instrument (Particle Sizing Systems, Santa Barbara, CA) equipped with a 633 nm He–Ne. An average Z-potential of  $-27 \text{ mV}$  was obtained by repeating the measurement on various AuNP solutions obtained by LASiS, similarly to what previously reported in the literature.<sup>43,46</sup> AuNP concentration was estimated by the Mie–Gans model fitting of UV-Vis spectra, as previously reported.<sup>42</sup> This method was tested on tens of AuNP solutions with different average size and aggregation levels.<sup>42</sup> The fitting model requires only three parameters: (i) the average radius of the nanoparticles ( $R$ ); (ii) the standard deviation ( $\sigma_G$ ) of a Gaussian function used to describe the statistical distribution of spheroid aspect ratios; and (iii) the fraction of spherical to spheroidal gold nanoparticles. For AuNP the dielectric constant of gold reported by Palik (E. D. Palik, *Handbook of Optical Constants of Solids*, Academic Press, New York, 1985), corrected for the size, was used, and water was considered as the dielectric host medium. The accuracy of the Mie–Gans model for the estimation of the average size of AuNP in water is of the order of 6% by using the calibration of the size dependent dumping frequency reported in ref. 42. The fitting program can be freely downloaded at [www.chimica.unipd.it/vincenzo.amendola](http://www.chimica.unipd.it/vincenzo.amendola).

Quantitative compositional analyses of samples were performed by inductively coupled plasma-mass spectrometry (ICP-MS). Measurements were carried out with a quadrupole based inductively coupled plasma-mass spectrometry (ICP-MS—Thermo Elemental X7 Series) equipped with the PlasmaLab software package. For instrument calibration, a standard Au solution was purchased from Spectrascan. Standard solutions for calibration of instrument were prepared by diluting the stock solutions to specified concentrations in de-ionized water (18.2 M $\Omega$ , Millipore, USA) and 2% HNO<sub>3</sub> (v/v) (Fluka). We compared the concentration of AuNP obtained by the MG fitting of the UV-visible spectra with the AuNP concentration obtained by ICP-MS measurement of gold atoms concentrations, by using the average particle size obtained by the MG-fit and the bulk gold atomic density. We analysed five solutions of AuNP with different average sizes and aggregation levels and we found an average error of 4%, with a maximum error of 8% and a minimum error of 1%.

### Raman analysis

The micro-Raman measurements were recorded on the SERS label solutions by focusing the  $5\times$  objective (NA 0.12, 36% coverage) of a Renishaw InVia micro-Raman instrument (CCD

detector with 100  $\mu\text{m}$  slits) on the middle of a 2 mm optical path quartz cuvette and using the 633 nm line of an He–Ne laser with output power of 13 mW. The Raman signal collected on an internal silicon chip was used every time to account for small (less than 5%) intensity fluctuations of the Raman spectrometer. Acquisition times were varied in the 10–600 s range in order to maximize the signal to noise ratio. Lysates were placed in a cylindrical well (3 mm diameter per 2 mm depth) coated with a microscope slide and analysed with the same experimental conditions: 5 $\times$  objective, the 633 nm line of an He–Ne laser and output power of 13 mW. Analysis on single fixed cells was performed with a 50 $\times$  objective and 1.3 mW laser power.

The Raman bands of SERS labels were fitted with a Lorentzian curve, according to what reported in ref. 13 in order to obtain a more accurate comparison.

### Cell culture and uptake experiments

U937 cells were obtained from the American Type Culture Collection and maintained according to ATCC protocols. The human non-adherent monocyte-like U937 cells were differentiated into macrophages by a 48 hours exposure to PMA (phorbol 12-myristate 13-acetate, Sigma-Aldrich) at a concentration of 40 nM. At day 0 cells were plated 0.5  $10^6$  cells per well in a 6 well plate and treated with PMA; after 48 hours the medium was changed and the cells resuspended in complete medium without PMA. At day 3 the uptake experiments were performed; briefly, cells were incubated in complete medium at 37  $^\circ\text{C}$  for two different time lengths (5 and 10 hours) with 2 nM final concentration of three different NP preparations (NP-MG, NP-CV and a 1 : 1 mix of NP-MG + NP-CV). A mock treated control well was also prepared. At the end of the incubation procedure, each well was washed four times with phosphate buffered saline medium (PBS) to eliminate the non-internalized NP and adherent cells were detached in PBS solution with a cell scraper. The cells obtained from each experimental point were subsequently counted in a Neubauer chamber, centrifuged for 5 minutes at 1000 rpm and resuspended at the same cells concentration ( $1.25 \times 10^5$  cells  $\text{ml}^{-1}$ ) in lysis buffer solution (Tris 50 mM pH = 8.0, NaCl 100 mM, EDTA 2 mM, Triton X-100 1%). Samples were stirred by vortex, incubated for 30 minutes at 0  $^\circ\text{C}$  and centrifuged (13 000 rpm, 20 minutes); then the protein concentration of each supernatants was estimated by the BCA methods (Pierce). Only slight differences in protein concentration between each sample were observed, which confirmed that cell lysates were obtained working with the same cells per volume ratio.

## Results and discussion

### Synthesis of SERS labels

SERS labels are based on AuNP synthesized by laser ablation synthesis in solution (LASIS), coated with polyethylene glycol (PEG) and functionalized with dye molecules (Fig. 1a). We mixed a 2 nM solution of 19 nm AuNP at a 100 : 1 volume ratio with freshly prepared 1 mM (in ethanol or in water) of 8 different types of dyes. These molecules are all commercially available and consist of 8 cationic dyes: methylene blue (BM), cresyl violet 670 (CV), hexacyanin 3 (HITC), malachite green (MG), malachite

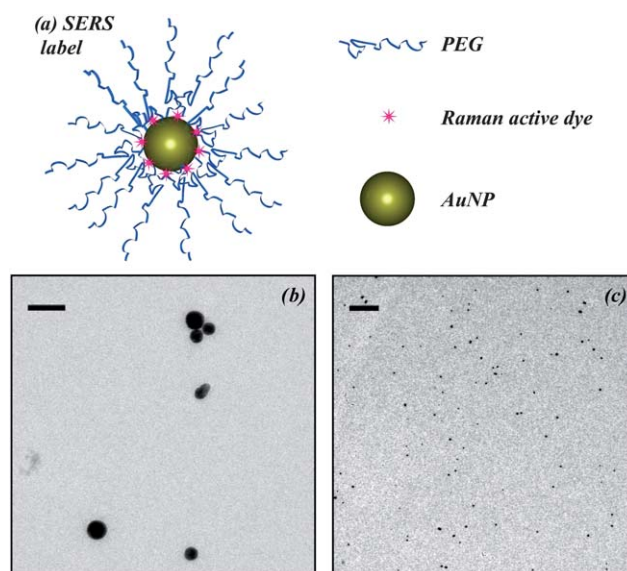


**Fig. 1** (a) Sketch of the SERS labels based on AuNP coated with PEG and functionalized with Raman active dye molecules. (b and c) Representative TEM images of pegylated AuNP loaded with MG dyes. Left: scale bar 100 nm. Right: scale bar 1  $\mu\text{m}$ .

green isothiocyanate (MGITC), Nile blue A (NB), oxazine 750 (OX), tetramethylrhodamine isothiocyanate (TRITC). Since AuNPs are negatively charged, as verified by Z-spectroscopy analysis, the dyes are linked to the particle surface by electrostatic interactions.<sup>19,32</sup> After 30 minutes of incubation, we added thiolated polyethylene glycol (PEG,  $M_w$  5000). Excess PEG and unbound dyes were removed by centrifugation after being incubated for 12 h. All Raman labels were obtained with the same procedure described above.

PEG capping conferred excellent stability to AuNP as well as to the dyes adsorbed on particles surface, as already reported by Nie's group. We also verified that the SERS labels can be obtained with a mixture of thiolated polyethylene glycol and bifunctional thiolate carboxylated polyethylene glycol or other multifunctional thiolated PEGs, in order to provide functional groups for bioconjugation. We added a concentration of dyes about 20 times larger than that used by Nie's group, and we did not observe important aggregation by TEM analysis (see for instance Fig. 1b and c). The coating of AuNP with PEG does not occur immediately after mixing and the incubation time of AuNP in the presence of excess PEG molecules is an important parameter for the preparation of efficient SERS labels. Incubation times shorter than about 2 hours do not allow a satisfactory coating of AuNP with PEG and negative effects on their stability in solution are observed. Incubation times longer than about 24 hours have negative effects on the intensity of the Raman signal of the SERS labels, probably due to the replacement of dye molecules with thiolated PEG on AuNP surface. We found that the optimum incubation time at room temperature is of the order of 10–15 hours for PEG : AuNP ratio of 15 000 : 1. We did not detect the absorption band of the dyes in the UV-visible spectra of the SERS labels, therefore we estimated that less than 200–100 dye molecules were present for single AuNP (see for example

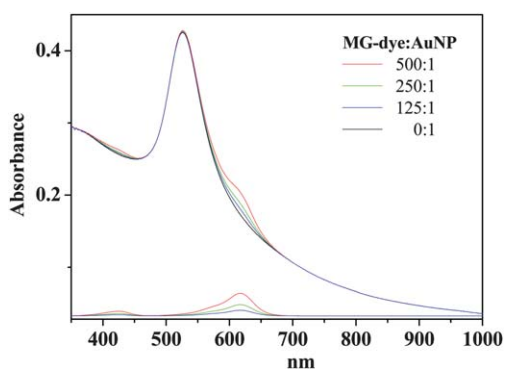


**Fig. 2** Superposition of the UV-visible spectra of AuNP in water (black line) and of the MG dye with variable molecules to gold nanoparticles ratio. The presence of the dye cannot be reliably determined for a ratio of MG dye to AuNP lower than about 125 : 1. Here we reported the case of the MG dye because it has an absorption band well separated from the plasmon band of AuNP, and therefore it is more visible than other more blue shifted dyes when superimposed to the plasmon band.

Fig. 2). It means that we have a dye concentration lower than 200–100 nM for a 2 nM solution of AuNP.

### Quantitative study of SERS tags

The concentration of AuNP after the functionalization process was measured by fitting the UV-visible spectra of particles solution with the Mie–Gans model (Fig. 3). The fitting is based on the Mie model for the extinction cross-section of spherical particles and accounts for the presence of small aggregates or non-spherical AuNP in solution by the Gans model for spheroids.<sup>42,47</sup> It has been successfully applied to aqueous solutions of AuNP with an accuracy of 6% on the nanoparticles average size with respect to sizes measured by transmission electron microscopy (TEM).<sup>42</sup> The accuracy of the method for the determination of particles concentration is on the order of the 4%, as tested by direct comparison with inductively coupled plasma mass spectrometry (ICP-MS) analysis on the same AuNP solutions. We previously showed that the Mie–Gans fitting model can be applied also to silver nanoparticles<sup>48</sup> and that the model can be extended to metal-dielectric core-shell structures by using the appropriate extension of the Mie model for layered spheres,<sup>49</sup> while the Gans model can be used for SERS labels based on nanorods.<sup>50</sup> Therefore, with slight modifications, the fitting

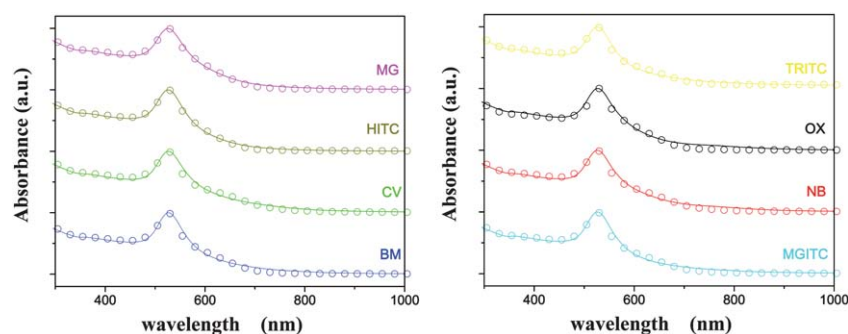


**Fig. 3** UV-visible spectra (straight lines) and Mie–Gans fitting (hollow circles) of the 8 SERS labels solutions. Fitting parameters are reported in the table. The meaning of the three parameters is described in the Experimental section.

model can be applied to a variety of commonly studied SERS tags.

Raman measurements on the solutions of SERS labels have been carried out in 2 mm optical path quartz cuvettes with a micro-Raman spectrometer equipped with a 5× objective and a He–Ne laser source at 633 nm and 13 mW of output power. In Fig. 4 one can clearly see that every SERS label has a distinctive fingerprint corresponding to the Raman spectrum of the dye adsorbed on particle surface, showing that the SERS tags we have considered are suited for multiplexed analysis.

The accurate determination of the AuNP concentration is a prerequisite for obtaining calibration curves between the Raman signal and the concentration of the SERS labels. We selected the most intense Raman bands for each of the 8 types of SERS labels (MG: 1614  $\text{cm}^{-1}$  peak, CV: 591  $\text{cm}^{-1}$  peak, NB: 1640  $\text{cm}^{-1}$  peak, OX: 1643  $\text{cm}^{-1}$  peak, BM: 1626  $\text{cm}^{-1}$  peak, TRITC: 1646  $\text{cm}^{-1}$  peak, and HITC: 795  $\text{cm}^{-1}$  peak). The calibration can be referred to the Raman peak intensity or integrated intensity. The latter case can be more useful when bands overlap and a fitting is necessary for peaks deconvolution. In both cases, fitting of the experimental data always showed a linear dependence between signal intensity and labels concentration, as expected. In Fig. 5 one can see that the brighter SERS labels can be detected at a concentration as low as few picomoles per litre. The noise thresholds in our experimental conditions were reported in Fig. 5 for three different acquisition times of 1, 10 and 100 s, in order to show that 100 s were enough to detect picomolar concentrations of the brighter SERS labels. When considering the volume probed by the focus of the 5× objective, that is of the order of 3000  $\mu\text{m}^3$ , one finds that about ten SERS labels are required to obtain a signal clearly detectable above the noise level with acquisition times of 100 s.

In order to better investigate the ability to discriminate the Raman fingerprints of different SERS labels, that is a prerequisite for their application in multiplex analysis, the intensity of the Raman bands of a mixture of different SERS tags has been measured for increasing dilution of one tag in the presence of a constant concentration of another tag. We found that the signal of the SERS labels was well detectable and still in the linearity regime for a ratio of the order of 1 : 50 between the diluted tag and the reference tag (Fig. 6).

The reproducibility of the Raman signal in SERS labels obtained from different batches is a recurrent problem.<sup>4,6,18,19,25,27,32,40</sup> We observed a relevant variability on the

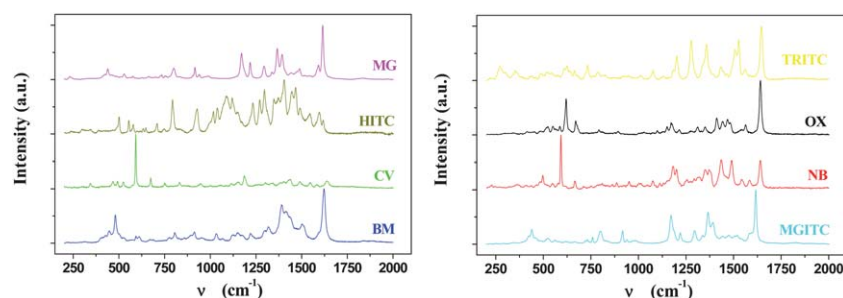


Fig. 4 Raman spectra of the 8 SERS labels (for details see text and Experimental section).

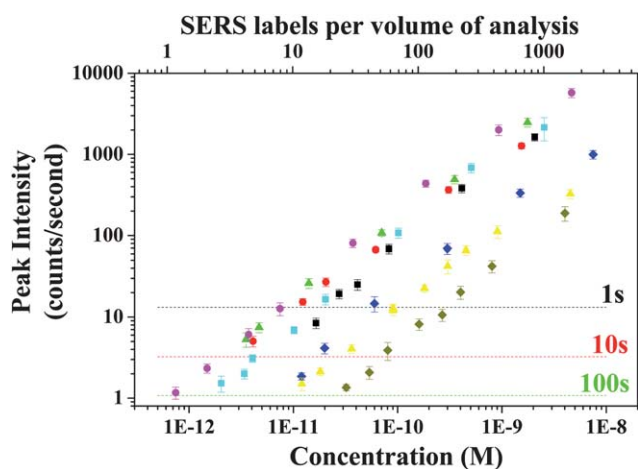


Fig. 5 The correlation between the intensity of the most intense Raman peaks and the concentration of 8 SERS labels (or the number of labels in the volume probed by the laser): BM ( $1626\text{ cm}^{-1}$  peak, blue diamonds), CV ( $591\text{ cm}^{-1}$  peak, green triangles), H1TC ( $795\text{ cm}^{-1}$  peak, khaki diamonds), MG ( $1614\text{ cm}^{-1}$  peak, magenta circles), MGITC ( $1618\text{ cm}^{-1}$  peak, cyan squares), NB ( $1640\text{ cm}^{-1}$  peak, red circles), OX ( $1643\text{ cm}^{-1}$  peak, black squares), TRITC ( $1646\text{ cm}^{-1}$  peak, yellow triangles). Noise thresholds in the experimental conditions for 1 s (black), 10 s (red) and 100 s (green) acquisition times are reported as dashed lines.

intensity of the Raman signal for SERS labels loaded with the same dye but prepared in different batches (Fig. 7a). Also ageing of SERS labels with the consequent decrease of the Raman signal over a period of weeks was observed (Fig. 7b). The latter effect can be likely due to the slow release of dye molecules from the surface of the SERS labels. Therefore, the application of SERS labels for quantitative analysis requires that the calibration curves are obtained with labels derived from the same batch and the same day of the analysis. In this context, the Mie–Gans fitting model is very useful because it requires few minutes for the evaluation of particles concentration by fitting their UV-visible spectrum.

### Nanoparticles uptake in macrophages

To demonstrate the reliability of this method for a working analytical application, we considered the problem of *in vitro* cell uptake of nanoparticles. We selected PMA differentiated U937 human cells because macrophage cells represent an efficient model for particles phagocytosis and we measured the Raman

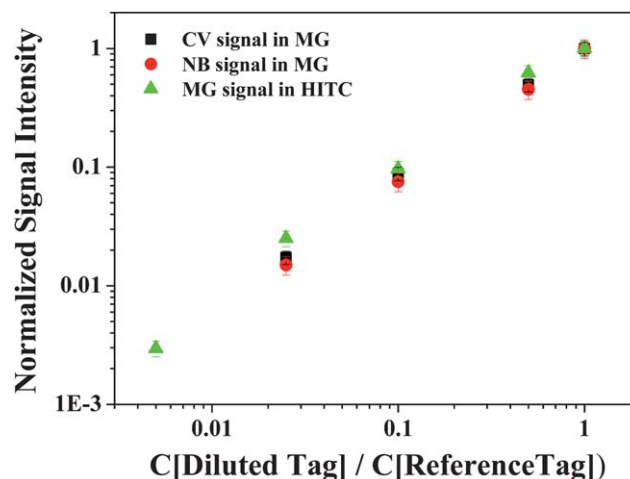
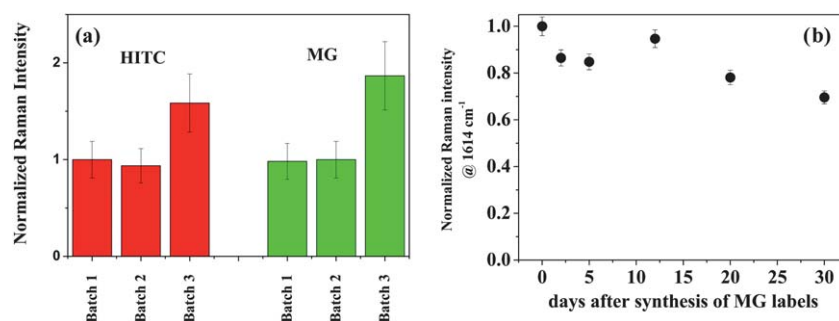


Fig. 6 The normalized Raman signal for 3 different SERS labels is reported in function of their relative dilution with respect to a reference label: CV label ( $591\text{ cm}^{-1}$  band) diluted in the presence of a constant concentration of MG label (black squares); NB label ( $593\text{ cm}^{-1}$  band) diluted in the presence of a constant concentration of MG label (red circles); MG label ( $1614\text{ cm}^{-1}$  band) diluted in the presence of a constant concentration of H1TC label (green triangles).

signal for the quantification of the SERS labels uptaken by macrophages at various times (5 and 10 hours) in cell lysates. The uptake of nanoparticles by cells and the detection of Raman signal from inside cells are topics of interest in drug delivery processes, in tracking of injected immunological cells to analyse their routing (e.g. tracking T cells), in the study of cell biology mechanisms and for diagnostic and therapeutic applications.<sup>26,51–57</sup> The uptake of particles by macrophages is interesting also for using cells as Trojan horse for delivering functional nano-materials into tissues that cannot be reached by the haematic flux or by external probes, as demonstrated with silica–gold nano-shells for photothermal therapy.<sup>58</sup>

We tested the quantitative SERS labels assay with two types of tags loaded with two different Raman active molecules: malachite green and cresyl violet. The strongest Raman bands of these two dyes do not overlap and, therefore, they can be used simultaneously. The stability of the Raman signal in the physiological medium, in the presence of the cytosol and in the presence of lysing agents, is a crucial parameter for absolute quantitative assays based on SERS labels. In fact, dye molecules are adsorbed on AuNP by electrostatic interactions and they can



**Fig. 7** We measured different  $d\sigma_R/d\Omega$  for the same type of SERS labels prepared in different batches ((a)—MG and HITC type labels considered in the figure) and a slow decrease of the Raman signal over a period of weeks ((b)—MG type label in the figure). Therefore quantitative measurements by SERS labels must be performed on labels from the same batches and with same ageing history.

be released through the PEG shell in the presence of highly saline solutions.<sup>19,32</sup> We investigated this point by 24 hours incubation of our labels in the presence of three common cell lysing agents, that are sodium dodecyl sulfate (SDS, anionic), cetyl trimethylammonium bromide (CTAB, cationic) and Triton X-100 (nonionic). We observed a large decrease of the Raman signal in all cases except than in the presence of Triton X-100 that is the only nonionic surfactant (Fig. 8a). It is likely that the ionic strength of the environment can induce the loss of a part of the cationic dye molecules bound to nanoparticles surface, with the consequent decrease of their SERS activity. A similar effect is observed by performing the same experiment in PBS solutions (Fig. 8b). In the light of these results, we used Triton X-100 as lysing agents for macrophage cells and we performed the calibration measurements by mixing the SERS labels with the same lysate solutions (containing PBS, cytosol and the lysis agents) that are present in our analytes.

For what concerns the uptake procedure, we incubated macrophage cells with AuNP loaded with the first (MG) or the second label (CV) and with a 1 : 1 mixture of the two SERS labels, at a concentration of about 2 nM, in order to test the reliability of the quantitative assay based on the intensity of the Raman signal. Incubations were performed at 37 °C in a CO<sub>2</sub> incubator for two different time lengths, 5 and 10 hours. After incubation, cells were thoroughly rinsed in order to remove non-internalized nanoparticles and detached from the culture plate. Then cells were counted in a Neubauer chamber and lysed with a lysis buffer solution containing 1% Triton X-100 at a cells per

volume ratio of  $1.25 \times 10^5$  cells ml<sup>-1</sup>. The lysis procedure was exploited for transforming the macrophage cells into a solution containing the AuNP based SERS labels, in order to correlate the Raman signal to the amount of uptaken nanoparticles by calibration curves similar to those reported in Fig. 5. The Raman analysis was repeated multiple times on lysate aliquots of 19  $\mu$ l from a reservoir of *ca.* 1 ml, whose protein concentration estimated by the BCA method was  $0.46 \pm 0.06$  mg ml<sup>-1</sup>, placed in a stainless steel well coated with a microscope slide. In all cases we detected a sharp signal that was correlated to SERS labels concentration by a calibration curve obtained for each SERS labels in the same experimental conditions (Fig. 9a) and diluted in the same matrix consisting of a lysate of cells of the same type but not incubated with nanoparticles.

Experimental results (Fig. 9b and c) indicate that in both cases a similar amount of MG and CV SERS labels were uptaken by macrophages, on the order of thousands of nanoparticles per cell per hour. This is in agreement with the expected results, because both the MG and CV SERS labels have an external PEG shell, therefore they are identical for macrophage cells but have different Raman fingerprints. The number of particles per cell is in agreement with previous reports about uptake processes in *in vitro* experiments with different cell lines.<sup>54,55</sup> Remarkably, these figures correspond to a concentration of AuNP in the samples of the order of 1–10 pM and to a number of AuNP in the volume probed by the Raman analysis of the order of 10 AuNP, because our samples contained approximately  $10^5$  cells ml<sup>-1</sup>. An independent measurement of the amount of AuNP uptaken by

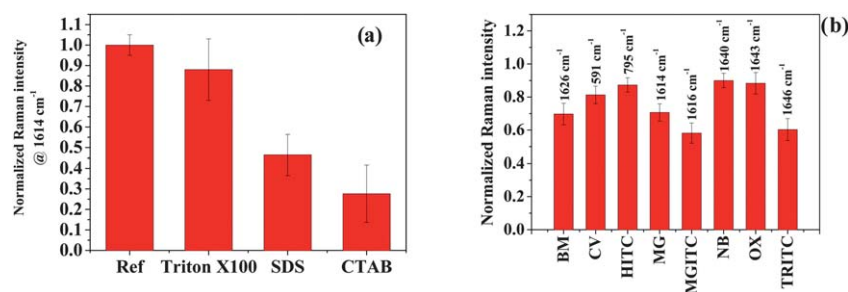


**Fig. 8** (a) The effect of ionic and nonionic surfactants on the intensity of the Raman signal of SERS labels (MG type labels considered in the figure) showed that ionic surfactants are detrimental for SERS performances. Solutions were incubated for 24 hours at room temperature. (b) The effect of PBS on the Raman signal of some representative SERS labels. Solutions were incubated for 24 hours at room temperature. These results suggest that quantitative measurements by SERS labels must be performed on labels in the same solution of the sample to be analyzed (cell lysates in our case).

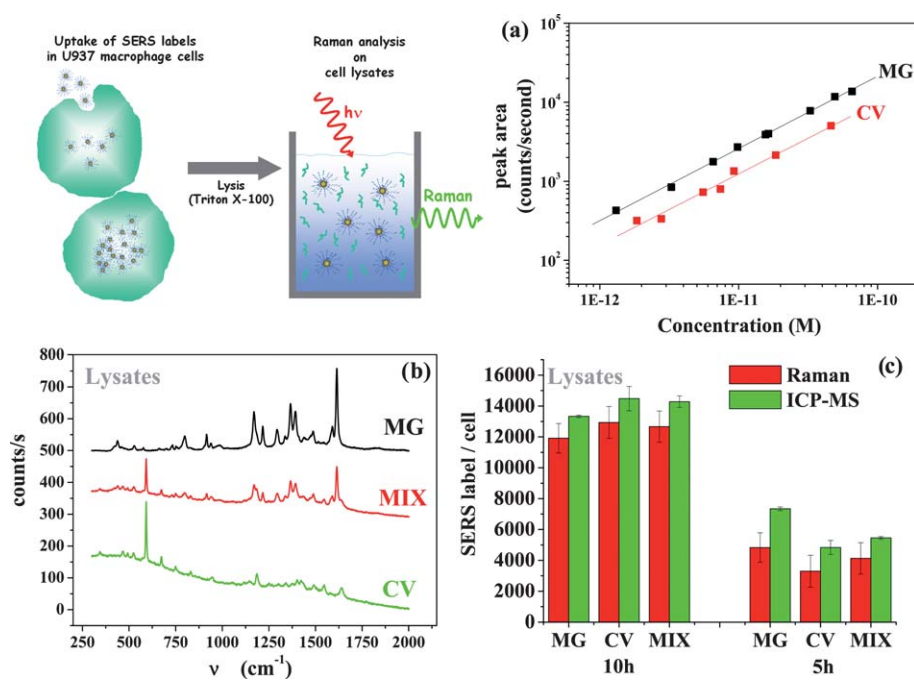


**Fig. 9** (a) Sketch of the procedure followed for the Raman analysis on SERS labels uptaken by macrophages and calibration curves of the two SERS labels used for uptake studies. Measurements were performed by diluting SERS label solutions at a ratio of 1 : 4 with cell lysate solutions. (b) Raman spectra collected on lysates of cells incubated with MG type (black), CV type (green) and a 1 : 1 mixture (MIX) of CV and MG types (red) SERS labels for 10 hours. (c) The average number of SERS labels uptaken by macrophage-differentiated U937 cells after incubation times of 5 h and 10 h evaluated by Raman spectroscopy (red bars) and by ICP-MS (green bars).

cells was carried out using ICP-MS. The results show an underestimation of the number of SERS labels per cell of  $\sim 20\%$  by Raman analysis with respect to ICP-MS analysis (Fig. 9c). The underestimation of the amount of SERS labels could be explained with the slow release of Raman reporters from the surface of AuNP in physiological medium, and can be avoided using more robust SERS labels like, for instance, labels obtained with thiolated dyes that are chemically bound to AuNP surface and/or encapsulating AuNP in silica shells.<sup>18,20–38</sup>

These results confirmed that the method for the quantification of SERS labels based on UV-visible spectroscopy is reliable for biological applications in physiological medium. This new analytical approach required both small volumes (less than 20  $\mu\text{l}$ ) and small amounts of tissues per cells (about 25 000).

## Conclusions

In summary, we showed a procedure for the quantification of SERS active gold nanoparticles by calibrating the Raman signal intensity with the concentration of SERS labels. The method exploits the fitting of the UV-visible spectrum of AuNP based SERS labels with the Mie–Gans model. The time stability of Raman signal in physiological medium and the reproducibility of the synthetic procedure are crucial parameters for quantitative applications of SERS labels. We applied the method to the quantification of the AuNP uptaken by macrophage cells and obtained good correlation with ICP-MS measurements. The quantitative measurement of Raman signal from SERS labels can open the way to ultrasensitive quantitative multiplexed

analysis and labelling of biomarkers down to picomolar concentration.

## Acknowledgements

V.A. and M.M. thank the University of Padova. M.C. gratefully acknowledges financial help from ABO Foundation, Fondazione Cariverona (Progetti Bando 2007), AIRC Regione Veneto.

## References

- 1 L. Wang, M. B. O'Donoghue and W. Tan, *Nanomedicine*, 2006, **1**, 413–426.
- 2 R. Wilson, A. R. Cossins and D. G. Spiller, *Angew. Chem., Int. Ed.*, 2006, **45**, 6104–6117.
- 3 R. A. Sperling, P. Rivera gil, F. Zhang, M. Zanella and W. J. Parak, *Chem. Soc. Rev.*, 2008, **37**, 1896–1908.
- 4 L. Sun, K. B. Sung, C. Dentinger, B. Lutz, L. Nguyen, J. Zhang, H. Qin, M. Yamakawa, M. Cao, Y. Lu, A. J. Chmura, J. Zhu, X. Su, A. A. Berlin, S. Chan and B. Knudsen, *Nano Lett.*, 2007, **7**, 351–356.
- 5 X. M. Qian and S. M. Nie, *Chem. Soc. Rev.*, 2008, **37**, 912–920.
- 6 W. E. Doering, M. E. Piotti, M. J. Natan and R. G. Freeman, *Adv. Mater.*, 2007, **19**, 3100–3108.
- 7 S. Wachsmann-Hogiu, T. Weeks and T. Huser, *Curr. Opin. Biotechnol.*, 2009, **20**, 63–73.
- 8 P. L. Stiles, J. A. Dieringer, N. C. Shah and R. P. Van Duyne, *Annu. Rev. Anal. Chem.*, 2008, **1**, 601–626.
- 9 W. Ruan, Z. Lu, T. Zhou, B. Zhao and L. Niu, *Anal. Methods*, 2010, **2**, 684–687.
- 10 Q. Chen, Y. Rao, X. Ma, J. Dong and W. Qian, *Anal. Methods*, 2011, **3**, 274–279.
- 11 S. Nie and S. R. Emory, *Science*, 1997, **275**, 1102.
- 12 K. Kneipp, H. Kneipp and J. Kneipp, *Acc. Chem. Res.*, 2006, **39**, 443–450.

- 13 E. C. Le Ru, E. Blackie, M. Meyer and P. G. Etchegoin, *J. Phys. Chem. C*, 2007, **111**, 13794–13803.
- 14 C. S. Allen and R. P. van Duyne, *Chem. Phys. Lett.*, 1979, **63**, 455–459.
- 15 M. Moskovits and D. P. Dilella, *Chem. Phys. Lett.*, 1980, **73**, 500–505.
- 16 J. R. Lombardi and R. L. Birke, *Acc. Chem. Res.*, 2009, **42**, 734–742.
- 17 H. Kneipp and M. Moskovits, *Surface-Enhanced Raman Scattering: Physics and Applications*, Springer Verlag, 2006.
- 18 E. S. Allgeyer, A. Pongan, M. Browne and M. D. Mason, *Nano Lett.*, 2009, **9**, 4784–4790.
- 19 X. Su, J. Zhang, L. Sun, T. W. Koo, S. Chan, N. Sundararajan, M. Yamakawa and A. A. Berlin, *Nano Lett.*, 2005, **5**, 49–54.
- 20 Y. C. Cao, R. Jin and C. A. Mirkin, *Science*, 2002, **297**, 1536–1540.
- 21 Y. C. Cao, R. Jin, J. M. Nam, C. S. Thaxton and C. A. Mirkin, *J. Am. Chem. Soc.*, 2003, **125**, 14676–14677.
- 22 D. Graham and K. Faulds, *Chem. Soc. Rev.*, 2008, **37**, 1042–1051.
- 23 L. Fabris, M. Dante, T. Q. Nguyen, J. B. H. Tok and G. C. Bazan, *Adv. Funct. Mater.*, 2008, **18**, 2518–2525.
- 24 D. C. Kennedy, K. A. Hoop, L. L. Tay and J. P. Pezacki, *Nanoscale*, 2010, **2**, 1413–1416.
- 25 C. Fernández-López, C. Mateo-Mateo, R. A. Álvarez-Puebla, J. Pérez-Juste, I. Pastoriza-Santos and L. M. Liz-Marzán, *Langmuir*, 2009, **25**, 13894–13899.
- 26 Y. Huang, V. P. Swarup and S. W. Bishnoi, *Nano Lett.*, 2009, **9**, 2914–2920.
- 27 B. Kustner, M. Gellner, M. Schutz, F. Schoppler, A. Marx, P. Strobel, P. Adam, C. Schmuck and S. Schlucker, *Angew. Chem., Int. Ed.*, 2009, **48**, 1950–1953.
- 28 M. Y. Sha, H. Xu, M. J. Natan and R. Cromer, *J. Am. Chem. Soc.*, 2008, **130**, 17214–17215.
- 29 S. Lee, S. Kim, J. Choo, S. Y. Shin, Y. H. Lee, H. Y. Choi, S. Ha, K. Kang and C. H. Ohs, *Anal. Chem.*, 2007, **79**, 916–922.
- 30 S. Keren, C. Zavaleta, Z. Cheng, A. de La Zerda, O. Gheysens and S. S. Gambhir, *Proc. Natl. Acad. Sci. U. S. A.*, 2008, **105**, 5844–5849.
- 31 C. L. Zavaleta, B. R. Smith, I. Walton, W. Doering, G. Davis, B. Shojaei, M. J. Natan and S. S. Gambhir, *Proc. Natl. Acad. Sci. U. S. A.*, 2009, **106**, 13511–13516.
- 32 X. Qian, X. H. Peng, D. O. Ansari, Q. Yin-Goen, G. Z. Chen, D. M. Shin, L. Yang, A. N. Young, M. D. Wang and S. Nie, *Nat. Biotechnol.*, 2008, **26**, 83–90.
- 33 G. von Maltzahn, A. Centrone, J. H. Park, R. Ramanathan, M. J. Sailor, T. A. Hatton and S. N. Bhatia, *Adv. Mater.*, 2009, **21**, 3175–3180.
- 34 J. Xie, Q. Zhang, J. Y. Lee and D. I. C. Wang, *ACS Nano*, 2008, **2**, 2473–2480.
- 35 W. Li, P. H. C. Camargo, X. Lu and Y. Xia, *Nano Lett.*, 2009, **9**, 485–490.
- 36 M. Sanles-Sobrido, W. Exner, L. Rodríguez-Lorenzo, B. Rodríguez-González, M. Correa-Duarte, R. A. Álvarez-Puebla and L. M. Liz-Marzán, *J. Am. Chem. Soc.*, 2009, **131**, 2699–2705.
- 37 A. Shen, L. Chen, W. Xie, J. Hu, A. Zeng, R. Richards and J. Hu, *Adv. Funct. Mater.*, 2010, **20**, 969–975.
- 38 F. McKenzie, K. Faulds and D. Graham, *Nanoscale*, 2010, **2**, 78–80.
- 39 D. S. Sebban, D. A. Watson and J. P. Nolan, *ACS Nano*, 2009, **3**, 1477–1484.
- 40 B. R. Lutz, C. E. Dentinger, L. N. Nguyen, L. Sun, J. Zhang, A. N. Allen, S. Chan and B. S. Knudsen, *ACS Nano*, 2008, **2**, 2306–2314.
- 41 G. Goddard, L. O. Brown, R. Habbersett, C. I. Brady, J. C. Martin, S. W. Graves, J. P. Freyer and S. K. Doorn, *J. Am. Chem. Soc.*, 2010, **132**, 6081–6090.
- 42 V. Amendola and M. Meneghetti, *J. Phys. Chem. C*, 2009, **113**, 4277–4285.
- 43 V. Amendola and M. Meneghetti, *Phys. Chem. Chem. Phys.*, 2009, **11**, 3805–3821.
- 44 V. Amendola and M. Meneghetti, *J. Mater. Chem.*, 2007, **17**, 4705–4710.
- 45 G. Compagnini, E. Messina, O. Puglisi and V. Nicolosi, *Appl. Surf. Sci.*, 2007, **254**, 1007–1011.
- 46 H. Muto, K. Yamada, K. Miyajima and F. Mafune, *J. Phys. Chem. C*, 2007, **111**, 17221–17226.
- 47 The fitting program can be downloaded freely at [www.chimica.unipd.it/vincenzo.amendola](http://www.chimica.unipd.it/vincenzo.amendola).
- 48 V. Amendola, S. Polizzi and M. Meneghetti, *Langmuir*, 2007, **23**, 6766–6770.
- 49 V. Amendola, G. A. Rizzi, S. Polizzi and M. Meneghetti, *J. Phys. Chem. B*, 2005, **109**, 23125–23128.
- 50 D. P. Sprunken, H. Omi, K. Furukawa, H. Nakashima, I. Sychugov, Y. Kobayashi and K. Torimitsu, *J. Phys. Chem. C*, 2007, **111**, 14299–14306.
- 51 J. Gunn, H. Wallen, O. Veisoh, C. Sun, C. Fang, J. Cao, C. Yee and M. Zhang, *Small*, 2008, **5**, 712–715.
- 52 S. Klein, S. Petersen, U. Taylor, D. Rath and S. Barcikowski, *J. Biomed. Opt.*, 2010, **15**, 036015.
- 53 M. J. Pittet, F. K. Swirski, F. Reynolds, L. Josephson and R. Weissleder, *Nat. Protoc.*, 2006, **1**, 73–79.
- 54 P. Nativo, I. A. Prior and M. Brust, *ACS Nano*, 2008, **2**, 1639–1644.
- 55 H. Jin, D. A. Heller, R. Sharma and M. S. Strano, *ACS Nano*, 2009, **3**, 149–158.
- 56 Q. Hu, L. Tay, M. Noestheden and J. P. Pezacki, *J. Am. Chem. Soc.*, 2007, **129**, 14–15.
- 57 A. Matschulat, D. Drescher and J. Kneipp, *ACS Nano*, 2010, **4**, 3259–3269.
- 58 M. R. Choi, K. J. Stanton-Maxey, J. K. Stanley, C. S. Levin, R. Bardhan, D. Akin, S. Badve, J. Sturgis, J. P. Robinson and R. Bashir, *Nano Lett.*, 2007, **7**, 3759–3765.